Original Paper

NeuroImmunoModulation

Neuroimmunomodulation 2017;24:231–241
DOI: 10.1159/000484931

Received: July 20, 2017
Accepted after revision: October 31, 2017
Published online: January 5, 2018

Suprachiasmatic Nucleus and Subordinate Brain Oscillators: Clock Gene Desynchronization by Neuroinflammation

Leila Maria Guissoni Campos[a, b] Rogerio Leone Buchaim[b, c]
Nathani Cristina da Silva[a] Caio Sergio Galina Spilla[b] Alessandre Hataka[d]
Luciana Pinato[a]

[a]São Paulo State University (UNESP) and [b]University of Marilia (UNIMAR), Marilia, [c]University of São Paulo (USP), Bauru, and [d]São Paulo State University (UNESP), Botucatu, Brazil

Keywords
Neuroinflammation · Circadian rhythms · Clock genes · Oscillators

Abstract
Objective: The clock genes Period *(per)* 1 and 2 are essential components in the generation and adjustment of biological circadian rhythms by the suprachiasmatic nucleus (SCN). Both genes are also rhythmically present in extrahypothalamic areas such as the hippocampus and cerebellum, considered subordinate oscillators. Several pathological conditions alter rhythmic biological phenomena, but the mechanisms behind these changes involving the clock genes are not well defined. The current study investigated changes in PER1 and PER2 immunoreactivity in the SCN, hippocampus, and cerebellum in a neuroinflammation model. ***Methods:*** Wistar rats received lipopolysaccharide (LPS) or vehicle intracerebroventricularly. The melatonin plasmatic content was quantified by ELISA to confirm the alterations in biological rhythms, and PER1 and PER2 immunoreactivities were analyzed in brain sections by immunohistochemistry. ***Results:*** In the SCN, intracerebroventricular LPS changed PER1 expression, increasing the number of PER1-immunoreactive (IR) cells at zeitgeber time (ZT) 15, decreasing it at ZT5 and ZT20 and not changing it at ZT10. LPS also induced a decrease in PER2-IR cells at ZT5, ZT10, and ZT15 but not at ZT20 in the SCN. In the hippocampus, LPS induced a decrease in PER1-IR and PER2-IR cells at both ZTs (ZT10 and ZT15). In the cerebellum, LPS increased the number of PER1-IR cells at ZT10 and decreased it at ZT15, while the number of PER2-IR cells was reduced at both ZTs. ***Conclusions:*** These results indicate that a neuroinflammatory condition leads to desynchronization of primary and subordinate brain oscillators, supporting the existence of the integration between the immune and the circadian system.

Introduction

The oscillatory capacity of the suprachiasmatic nucleus of the hypothalamus (SCN), the primary oscillator in the generation and regulation of circadian rhythms, involves transcription and translation feedback loops of its cells that result in the rhythmic expression of clock genes and their proteins [1]. The clock genes *per1* and *per2* exert a crucial role in this process of determining

E-Mail karger@karger.com
www.karger.com/nim

Leila Maria Guissoni Campos
UNIMAR, Câmpus Universitário
Av. Higino Muzi Filho 1001
Jardim Araxa, Marília, SP 17525-902 (Brazil)
E-Mail guissoni.campos@gmail.com

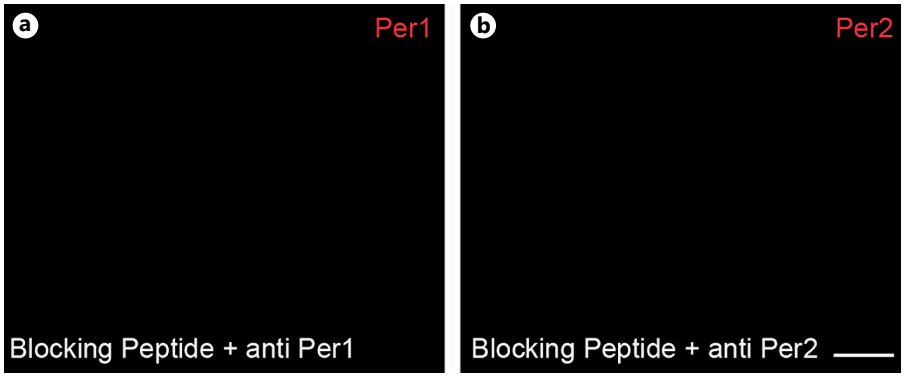

Color version available online

Fig. 1. Photomicrographs of brain frontal sections at hippocampus level, showing absence of the PER1 and PER2 protein expression after immunogenic peptide preadsorption and incubation with PER1 (E-8) blocking peptide (**a**), and PER2 (1-P) blocking peptide (**b**). Scale bar = 100 μm.

circadian behavioral rhythms [2]. PER proteins regulate their own transcription by means of a negative feedback loop between them and the nucleus, providing a post-translational component to the circadian clock mechanism [1].

The expression of circadian rhythms in physiology and behavior involves the participation of the circadian timing system and includes forebrain structures and the cerebellum [3], subordinate oscillators which, in normal conditions, can express different patterns of clock genes in close phase or in antiphase with the SCN rhythms [4, 5].

The ability of pathological conditions to alter clock gene expression in the SCN [6] and peripheral structures [7–9] is well known, resulting in desynchronization of rhythms such as sleep disorders, daily mood changes, hormone secretion disorders, thermoregulation changes, and locomotor activity phase changes [10, 11], which in turn can influence the pathological response itself [12].

Melatonin, a neuroendocrine transducer of photoperiod information and circadian rhythm regulator, decreases after intracerebroventricular injection of the bacterial endotoxin lipopolysaccharide (LPS) [13]. This condition is correlated with the activation of the pineal axis [14] and may represent one of the factors that influence the desynchronization of the clock genes.

Thus, to investigate whether a neuroinflammatory condition could change PER1 and PER2 protein expression in the primary and subordinate brain oscillators, in the present study, PER1 and PER2 protein expression levels were evaluated in the SCN, hippocampus, and cerebellum in a model of neuroinflammation induced by intracerebroventricular LPS injection. Although systemic doses of LPS may act on the clock [6], this effect is associated with its peripheral actions [7–9, 15]. Furthermore, in models of intraperitoneal injections, the blood-brain barrier is relatively resistant to LPS, leaving some regions more vulnerable than others to intraperitoneal injections [16]. To investigate the central effects of LPS in the SCN, hippocampus, and cerebellum in the present study, a neuroinflammatory model using intracerebroventricular injection was used. In addition, the plasmatic melatonin content of these animals was evaluated to verify the effect of LPS on the output rhythm of the SCN. Furthermore, quantification of cell death with the caspase marker was evaluated to demonstrate that the brain areas were affected by LPS since caspase function represents part of the innate immune response to an inflammatory environment [17].

Materials and Methods

All procedures included in this work comply with the ethical standards of the Guidelines for the Care and Use of Mammals in Neuroscience and Behavioral Research and were approved by the local ethics committee (proc. 001/2015). All efforts were made to minimize the number of animals and their suffering.

Intracerebroventricular LPS Injection

Adult male (P60) Wistar rats ($n = 40$) obtained from the central facility of São Paulo State University were housed under controlled conditions in a 12-h light:12-h dark cycle with lights on at 7:00 a.m., considered zeitgeber time 0 (ZT0), with controlled temperature and humidity and water and food (Nuvilab, Nuvital, Brazil) ad libitum.

The animals were subjected to surgery to implant a metal guide cannula (0.8 mm) in the left lateral ventricle [13]. After 7 days, 20 animals received sterile saline (5 μL, i.c.v.) (control group) and 20 received LPS (3 μg/5 μL, i.c.v.) (LPS group) (Sigma Chemical, St. Louis, MO, USA). Because the peak effect of LPS is between 1.5 and 4 h and declines after 8 h [18] and systemic LPS disturbs the *per1* rhythm in the SCN after 5 h [6], in the present study, PER1 and PER2 protein expression levels were evaluated 6 h after LPS. Animals were transcardially perfused ($n = 5$ per ZT) with saline

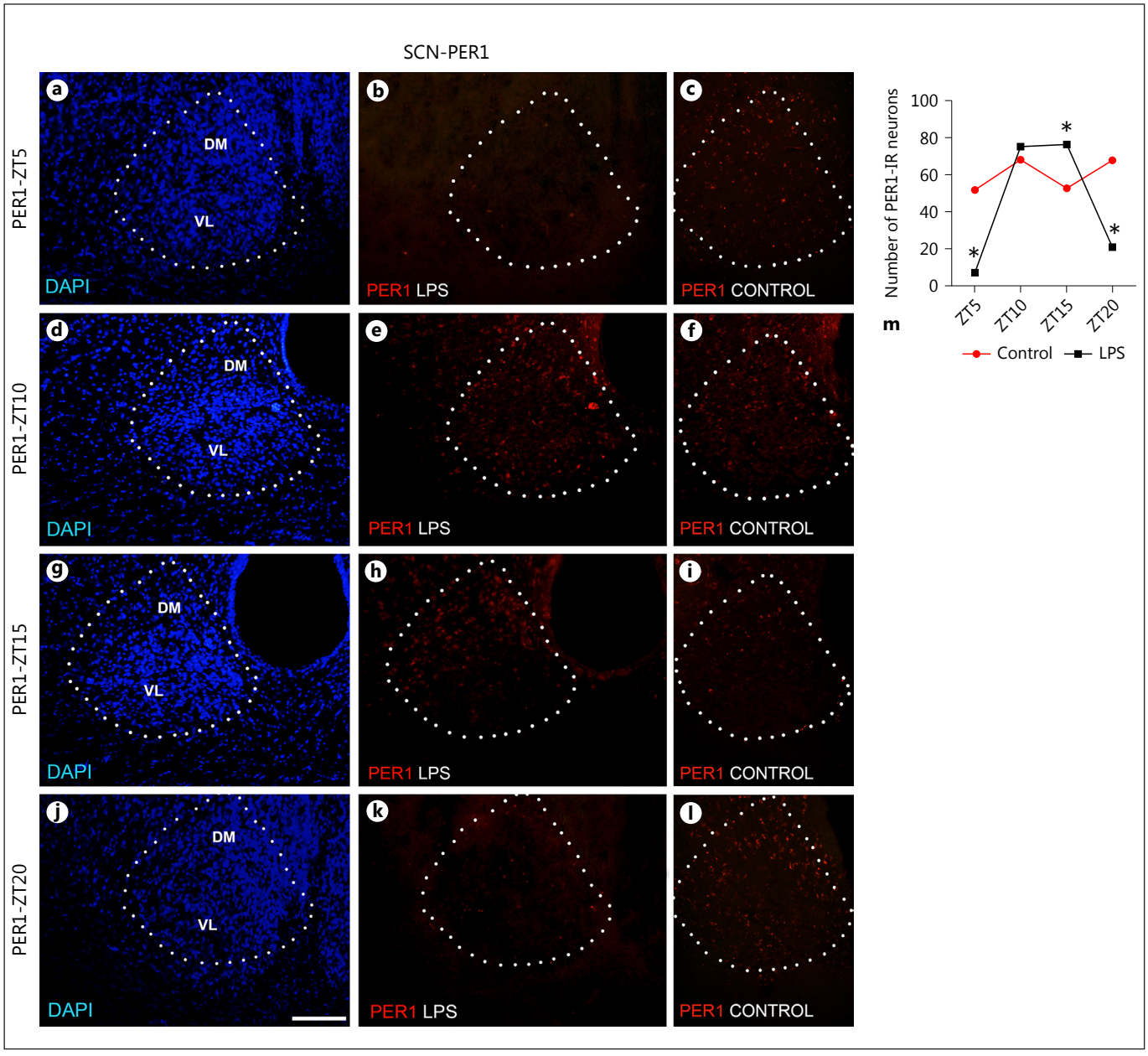

Fig. 2. Temporal variations in the distribution and in the number of PER1-IR cells in the suprachiasmatic nucleus (SCN) of rats injected intracerebroventricularly with saline (control) or LPS and perfused at different time points (ZT5, ZT10, ZT15, and ZT20). DM, the dorsomedial portion of the nucleus; VL, the ventrolateral portion of the nucleus. Photomicrographs of brain frontal sections showing PER1-IR cells (red) in the LPS group in 4 periods: ZT5 (**b**), ZT10 (**e**), ZT15 (**h**), and ZT20 (**k**). The same periods were used for the control group: ZT5 (**c**), ZT10 (**f**), ZT15 (**i**), and ZT20 (**l**). **a**, **d**, **g** and **j** The SCN cell nuclei indicating the nucleus boundaries by DAPI stain. **m** Quantification of immunohistochemical results showing the number of PER1-IR cells in the 4 analyzed ZTs ($n = 5$ animals per ZT). * $p < 0.05$: LPS significantly different compared to control. The data are expressed as the mean ± SEM. Scale bar = 100 μm.

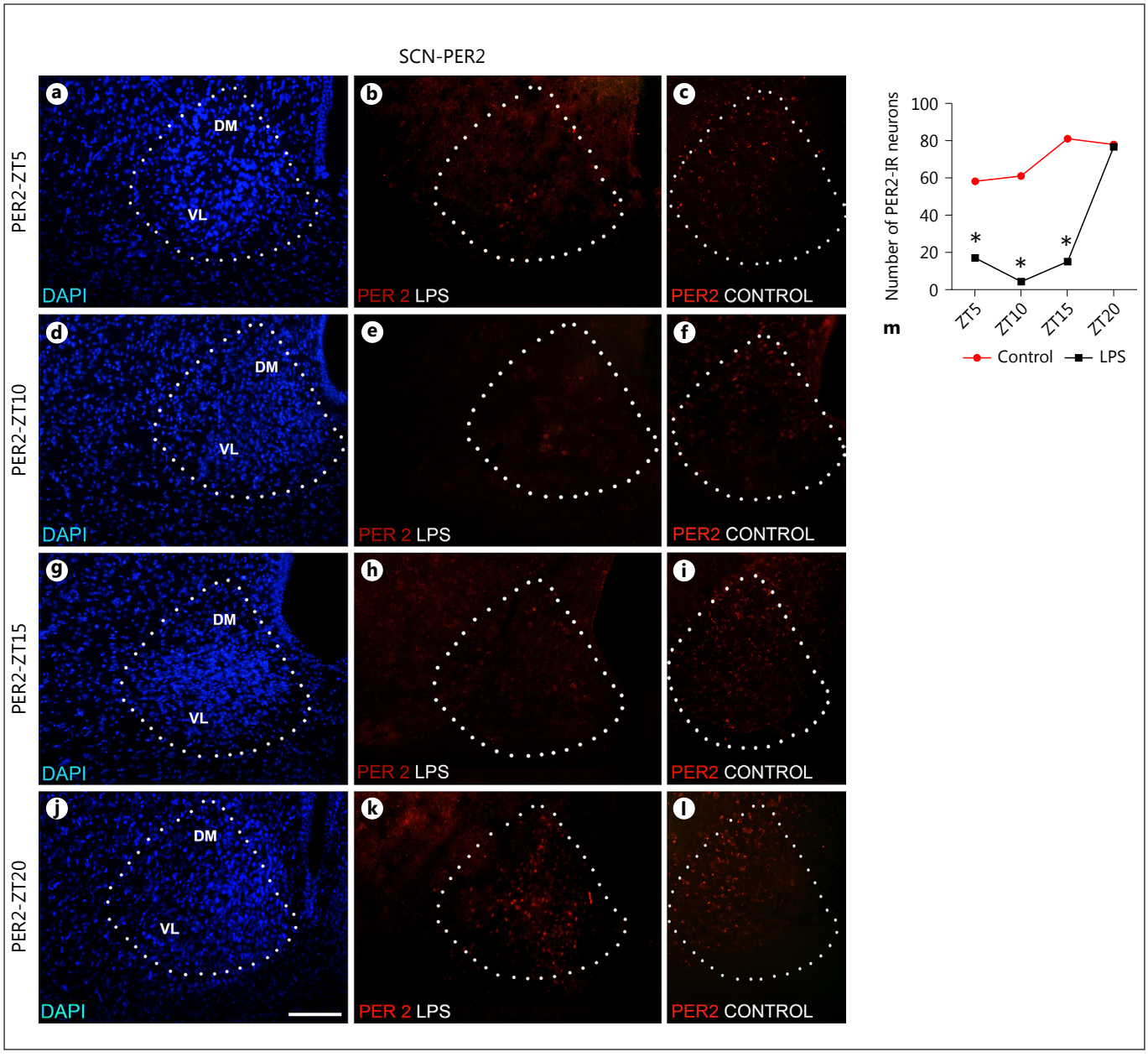

Fig. 3. Temporal variations in the number of PER2-IR cells in the suprachiasmatic nucleus (SCN) of rats injected intracerebroventricularly with saline (control) or LPS and perfused at different time points (ZT5, ZT10, ZT15, and ZT20). DM, the dorsomedial portion of the nucleus; VL, the ventrolateral portion of the nucleus. Photomicrographs of brain frontal sections showing PER2-IR cells (red) in the LPS group in 4 periods: ZT5 (**b**), ZT10 (**e**), ZT15 (**h**), and ZT20 (**k**). The same periods were used for the control group: ZT5 (**c**), ZT10 (**f**), ZT15 (**i**), and ZT20 (**l**). **a**, **d**, **g** and **j** The SCN cell nuclei indicating the nucleus boundaries by DAPI stain. **m** Quantification of immunohistochemical results showing the number of PER2-IR cells in the 4 analyzed ZTs (n = 5 animals per ZT). * $p < 0.05$: LPS significantly different compared to control. The data are expressed as the mean ± SEM. Scale bar = 100 μm.

Neuroimmunomodulation 2017;24:231–241
DOI: 10.1159/000484931

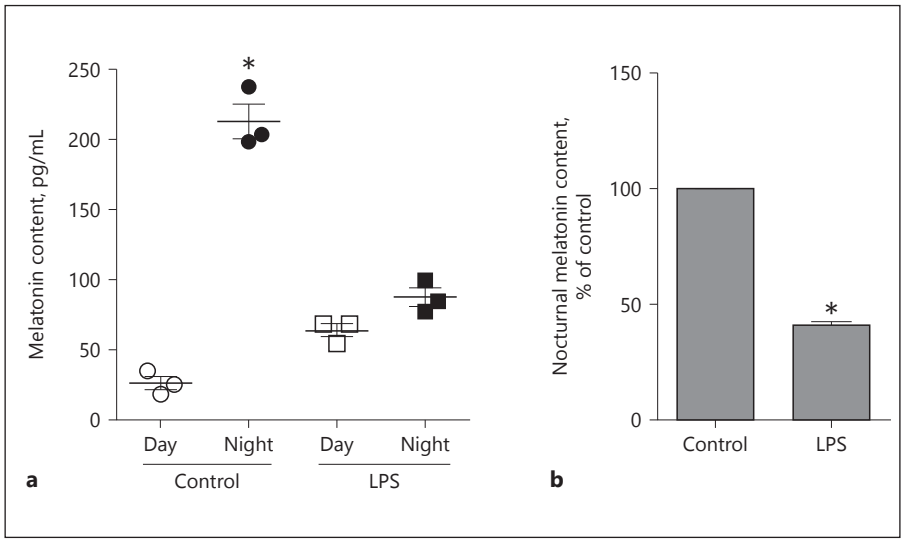

Fig. 4. Blockage of plasmatic melatonin following intracerebroventricular LPS. **a** Day and night plasmatic melatonin content (pg/mL) in rats injected intracerebroventricularly with saline (control) or LPS; * $p < 0.05$: significantly different comparing day and night. **b** Percentage in relation to control (100%) of plasma melatonin content in the dark phase in the LPS group (3 μg i.c.v., 6 h); * $p < 0.05$: significantly different compared to control. The data are expressed as the mean ± SEM. $n = 3$ per group.

(200 mL), followed by 300 mL of 4% paraformaldehyde at ZT5, ZT10, ZT15, or ZT20. Red lights were used during intracerebroventricular injection, anesthesia, and blood collection when they occurred during the dark phase. Blood collection was performed by means of cardiac puncture immediately prior to the transcardiac perfusion process.

Tissue Collection

Following the protocol described in Campos et al. [19], after transcardiac perfusion, the brains were cryoprotected and cryosectioned, and the 30-μm-thick sections were serially stored in 10 different stepwise antifreeze solutions. The coronal sections of one series representing the entire extent of the SCN, hippocampus, and cerebellum were placed in a rostrocaudal order. After this, sections representing the same rostrocaudal levels were processed for each antibody.

Immunohistochemistry

The free-floating brain sections were incubated in PER1 (1:200, Santa Cruz Bio, UK), PER2 (1:200, Santa Cruz Bio, UK), and caspase (1:200, Santa Cruz Bio, UK) primary antibodies for 24 h. After the sections had been rinsed in PBS-TX buffer (0.05 M), they were incubated in normal serum (2%) containing the fluorescent secondary antibody Cy3 (1:200, Jackson Immuno Research, UK) for 2 h. After this, cell nuclei were stained by 6-diamidino-2-phenylindole (DAPI) (Sigma Chemical), and the sections were analyzed by epifluorescence microscopy. The negative staining controls were performed by omitting the primary caspase antibody and with the addition of the PER1 (E-8) blocking peptide (Santa Cruz Biotechnology, sc-398890 P, TX, USA) and PER2 control/blocking peptide No. 1 PER2 (1-P) (Alpha Diagnostic International Inc., TX, USA) to the primary incubation solution of PER1 and PER2 antibodies, which blocked PER1 and PER2 staining (Fig. 1).

Plasma Melatonin Determination

The plasmatic melatonin content was determined using the enzyme-linked immunosorbent assay (ELISA) technique with commercial kits following the manufacturer's instruction (Tecan Trading AG, Switzerland). For this, the plasma for this measurement was collected from the heart (left ventricle) by puncture before the transcardiac perfusion process. The data are expressed as the mean ± SEM of plasma content (pg/mL) and in percentages of LPS group in relation to control, $n = 3$ per group.

Data Analysis

Each coronal section was analyzed under a light field and epifluorescence (Olympus BX50 microscope), and the images were acquired with cellSens software (USA). All visible cells immunoreactive (IR) for each antibody were counted in a series of brain sections ($n = 6$ sections per brain region, representing rostrocaudal levels of the SCN, hippocampus, and cerebellum) using ImageJ software (McMaster Biophotonics Facility, Canada). The data are expressed as the mean ± standard error of the mean of the PER1- and PER2-IR cell number counted per section in each ZT. The presence of caspase-IR cell bodies was individually evaluated through semiquantitative analysis among the positively labeled regions according to a previously defined rating scale in which + means low optical density; ++ means moderate, and +++ means high optical density.

The SCN sections of ZTs 5, 10, 15 and 20 and the cerebellum and hippocampus sections of ZTs 10 and 15 were analyzed. The analysis of variance followed by Newman-Keuls posttest was applied to compare among ZTs and groups.

Results

The PER1 and PER2 proteins presented variations in day/night expression patterns in the SCN, hippocampus, and cerebellum of the control rats. The hippocampus showed PER1 day/night variation in phase with the SCN unlike the cerebellum, which showed PER1 day/night variation in antiphase with the SCN. In contrast, the hip-

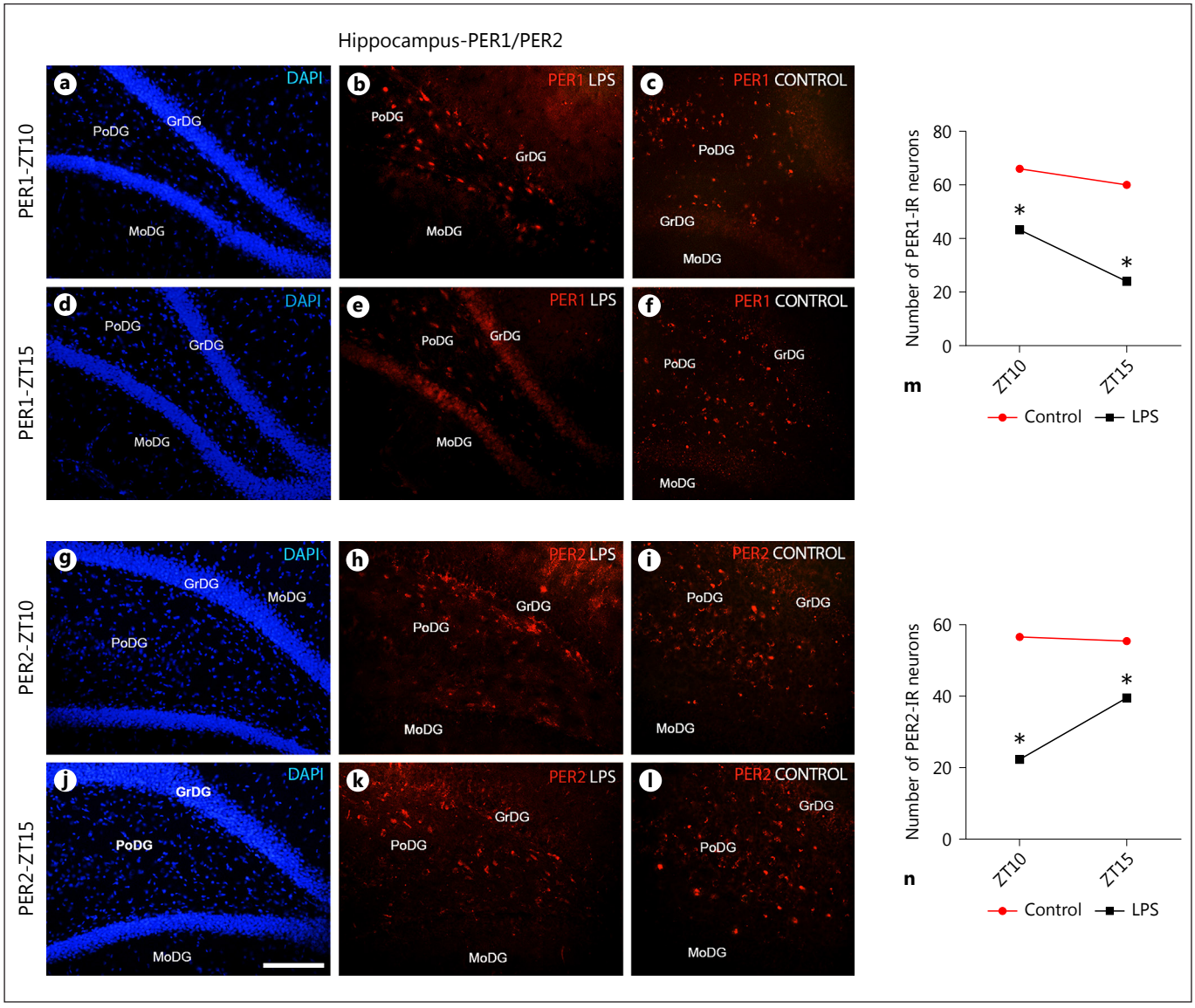

Fig. 5. Temporal variations (ZT10 and ZT15) in the number of PER1- and PER2-IR cells in the hippocampus of rats injected intracerebroventricularly with saline (control) or LPS. GrDG, dentate gyrus granular layer; PoDG, dentate gyrus polymorphic layer; MoDG, dentate gyrus molecular layer. Photomicrographs of brain frontal sections showing PER1-IR cells in the control group in 2 periods, ZT10 (**c**) and ZT15 (**f**), and in the LPS group also in 2 periods, ZT10 (**b**) and ZT15 (**e**), and PER2-IR cells in the control group in 2 periods, ZT10 (**i**) and ZT15 (**l**), and in the LPS group also in 2 periods, ZT10 (**h**) and ZT15 (**k**). **a**, **d**, **g** and **j** The hippocampus cell nuclei indicating the layer boundaries by DAPI stain. **m** Quantification of immunohistochemical results showing the number of PER1-IR cells. **n** The number of PER2-IR cells at the 2 analyzed ZTs ($n = 5$ animals per ZT). * $p < 0.05$: LPS significantly different compared to control. The data are expressed as the mean ± SEM. Scale bar = 100 μm.

pocampus did not show PER2 day/night variation, and the cerebellum showed PER2 day/night variation in phase with the SCN.

In the SCN, immunofluorescence analysis of PER1 and PER2 revealed different organizations of both proteins inside this nucleus depending on the ZT. When immunoreactivity was compared across ZTs, few PER1-IR cells were observed throughout the SCN in the LPS group at ZT5 (Fig. 2b) and ZT20 (Fig. 2k). At ZT10, PER1 was observed throughout the entire SCN both in the control and LPS groups (Fig. 2e, f). At ZT15, there were fewer PER1-IR cells in the control group than at ZT10 (ZT10

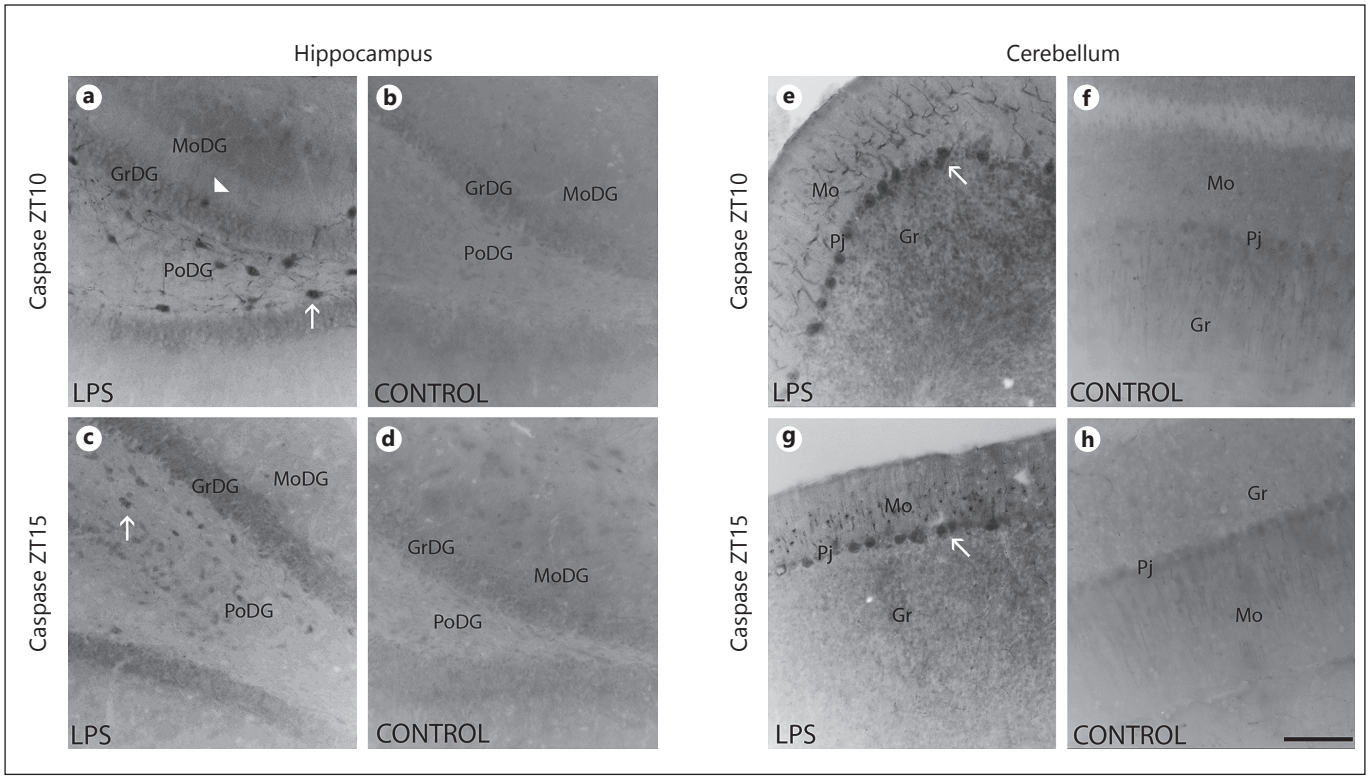

Fig. 6. Caspase: temporal variations (ZT10 and ZT15) in the number of caspase-positive cells in the dentate gyrus (DG) and cerebellum of rats injected intracerebroventricularly with saline (control) or LPS. Mo, molecular layer; Pj, Purkinje cell layer; Gr, granular layer; GrDG, granular layer; PoDG, dentate gyrus polymorphic layer; MoDG, dentate gyrus molecular layer. Representative caspase staining in DG coronal sections, from rats submitted to LPS treatment in ZT10 (**a**) and ZT15 (**c**), and controls in ZT10 (**b**) and ZT15 (**d**). Caspase-positive cells in the Purkinje cell layer (arrow) from rats submitted to LPS treatment in ZT10 (**e**) and ZT15 (**g**). Scale bar = 100 μm.

68.0 ± 3.0, ZT15 52.6 ± 7.1, $p < 0.001$) (Fig. 2h, i, m). At ZT20, there were more PER1-IR cells in the control group (ZT15 52.6 ± 7.1, ZT20 67.8 ± 3.7, $p < 0.001$) and fewer in the LPS group (21.0 ± 5.2, $p < 0.001$) than at ZT15 (Fig. 2k–m). When PER1 immunoreactivity was compared between the LPS and control groups, LPS increased PER1 expression at ZT15 (control 52.6 ± 7.1, LPS 76.3 ± 4.4, $p < 0.001$), did not change it at ZT10, and decreased it at ZT5 (control 51.8 ± 11.2, LPS 7.3 ± 3.2, $p < 0.001$) and ZT20 (control 67.8 ± 3.7, LPS 21.0 ± 5.2, $p < 0.001$) (Fig. 2m).

PER2 was mainly found in the dorsal part of the SCN at ZT15 and ZT20 in the control group (Fig. 3i, l). After LPS, the number of PER2-IR cells decreased at ZT5 (control 58.1 ± 5.9, LPS 17.2 ± 3.1, $p < 0.001$), ZT10 (control 61.0 ± 6.0, LPS 4.5 ± 1.4, $p < 0.001$), and ZT15 (control 81.0 ± 2.6, LPS 15.1 ± 4.9, $p < 0.001$) but not at ZT20 (Fig. 3m).

Besides the effects of LPS in the SCN, the analysis of the melatonin level showed a reduction in nocturnal plasmatic melatonin following LPS ($p < 0.05$), which suggests a desynchronization of this circadian rhythm (Fig. 4).

In the hippocampus, the control group showed a low density of PER1-IR and PER2-IR cells in the granular layer and strong staining for both proteins in the polymorphic layer (Fig. 5c, f, i, l). The LPS changed this pattern by increasing PER1-IR in the granular layer at ZT15 (Fig. 5e), although this change was not reflected in an increase in the total number of PER1-IR cells (Fig. 5e). LPS decreased PER1 expression at ZT10 (control 66.2 ± 3.9, LPS 43.3 ± 6.4, $p < 0.001$) and ZT15 (control 60.0 ± 4.9, LPS 24.0 ± 4.6, $p < 0.001$) (Fig. 5m). LPS also decreased the number of PER2-IR cells at ZT10 (control 56.6 ± 4.5, LPS 22.3 ± 2.5, $p < 0.001$) and ZT15 (control 55.5 ± 3.9, LPS 39.7 ± 3.7, $p < 0.001$) (Fig. 5n). The number of caspase-IR cells was increased in the polymorphic layer and granular layer of the dentate gyrus after LPS to a greater extent at ZT10 (Fig. 6a) than at ZT15 (Fig. 6c, Table 1).

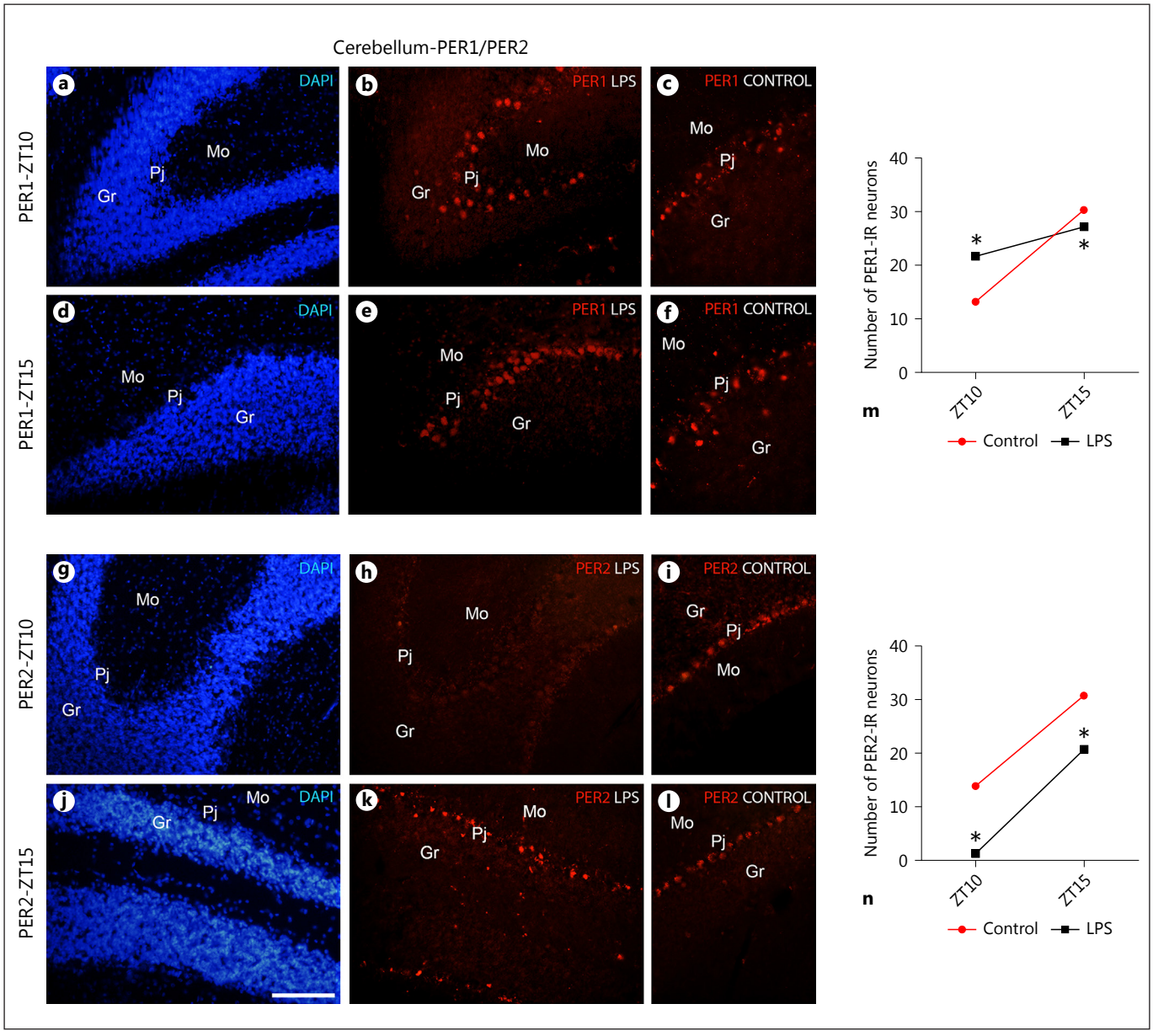

Fig. 7. Temporal variations (ZT10 and ZT15) in the number of PER1 and PER2-IR cells in the cerebellum of rats injected intracerebroventricularly with saline (control) or LPS. Mo, molecular layer; Pj, Purkinje cell layer; Gr, granular layer. Photomicrographs of brain frontal sections showing PER1-IR cells in the control group in 2 periods, ZT10 (**c**) and ZT15 (**f**), and in the LPS group also in 2 periods, ZT10 (**b**) and ZT15 (**e**), and PER2-IR cells in the control group in 2 periods, ZT10 (**i**) and ZT15 (**l**), and in the LPS group also in 2 periods, ZT10 (**h**) and ZT15 (**k**). **a**, **d**, **g** and **j** The cerebellum cell nuclei indicating the layer boundaries by DAPI stain. **m** Quantification of immunohistochemical results showing the number of PER1-IR cells. **n** The number of PER2-IR cells at the 2 analyzed ZTs ($n = 5$ animals per ZT). * $p < 0.05$: LPS significantly different compared to control. The data are expressed as the mean ± SEM. Scale bar = 100 μm.

In the cerebellum, PER1 and PER2 were found in the Purkinje cell layer with peak expression at ZT15 in the control group (Fig. 7f, l–n). LPS increased PER1 expression at ZT10 (control 13.2 ± 3.5, LPS 21.7 ± 3.4, $p < 0.001$) and decreased it at ZT15 (control 30.3 ± 4.2, LPS 27.2 ± 4.2, $p < 0.05$) (Fig. 5a–f, m). In contrast, LPS decreased PER2 expression at both ZTs (ZT10, control 13.8 ± 3.7, LPS 1.3 ± 1.5, $p < 0.001$; ZT15, control 30.7 ± 3.2, LPS 20.7 ± 3.5, $p <$

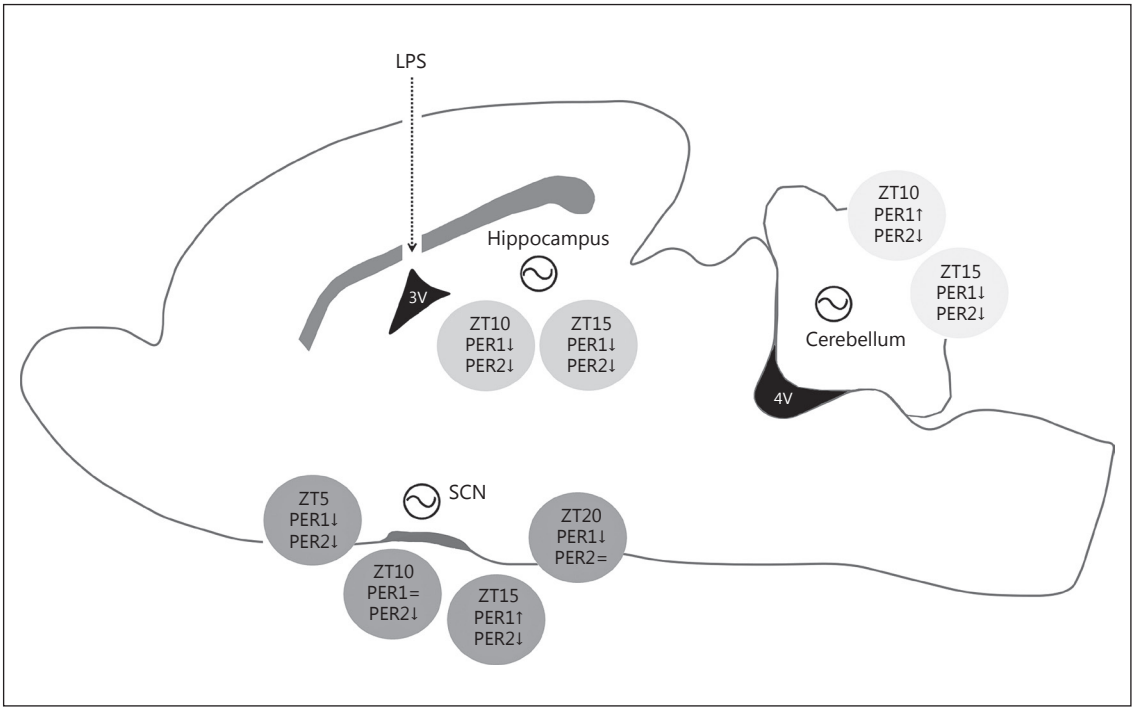

Fig. 8. Changes in the PER1 and PER2 following LPS. Schematic drawing of a sagittal slice of the rat brain summarizing the effects of neuroinflammatory stimulus with LPS (3 μg/5 μL i.c.v., 6 h) inducing changes in the expression of PER1 and PER2 proteins in the SCN, hippocampus, and cerebellum depending on the ZT analyzed. 3V, third ventricle; 4V, fourth ventricle; ZT, zeitgeber time.

Table 1. Caspase-IR cells

	LPS		Control	
	Z10	Z15	Z10	Z15
Hippocampus				
Granular layer	+	Ø	Ø	Ø
Polymorphic layer	+++	+	Ø	Ø
Molecular layer	Ø	Ø	Ø	Ø
Cerebellum				
Granular layer	Ø	Ø	Ø	Ø
Purkinje cell layer	+++	+++	Ø	Ø
Molecular layer	++	++	Ø	Ø

+, low density of caspase-IR cells; ++, moderate density of caspase-IR cells; +++, high density of caspase-IR cells; Ø, absence of caspase-IR cells.

0.001) (Fig. 7g–l, n). Caspase-positive cells were observed in Purkinje cells after LPS at ZT10 and ZT15 (Fig. 6e, g).

In summary, neuroinflammatory stimulation with LPS (3 μg/5 μL i.c.v., 6 h) induced changes in PER1 and PER2 expression in the SCN, hippocampus, and cerebellum depending on the ZT analyzed (Fig. 8).

Discussion

In agreement with our previous results [13], there was a reduction in plasmatic melatonin following intracerebroventricular injection of LPS, indicating the loss of the SCN rhythm and consequently the loss of the endocrine photoperiodic information and the protective action of this molecule [20].

The neuroinflammation induced by intracerebroventricular LPS in the present study resulted in changes in PER1 and PER2 expression in the SCN, hippocampus, and cerebellum dependent on the time analyzed. Previous studies had already demonstrated that systemic LPS significantly changed *per2* expression in the SCN [6]. In the present study, the susceptibility to LPS found in the SCN, hippocampus and cerebellum appeared to be dependent on the time of day in which the stimulus was applied. A day-night rhythm in the susceptibility to lethal

doses of LPS has already been demonstrated, and inflammation may directly affect the SCN, as suggested by the LPS-induced phase delays during the subjective night [21]. These time-dependent effects are reflected in several phenomena since LPS administration at the beginning of the active period induces severer responses in temperature and proinflammatory cytokines than LPS given in the rest period [22]. As a matter of fact, the evolution of the acute inflammatory environment occurs rapidly, when LPS induces substantially higher levels of cytokines with peak levels between 1.5 and 4 h, which begins to decline 8 h after administration [18]. Therefore, in the present study, we analyzed melatonin content, caspase, PER1 and PER2 expression 6 h after LPS administration.

The relationships between these mechanisms and clinical conditions are evident in clinical studies that have shown a correlation between the time of day and worsening illness manifestations [23]. In the present study, peak expression of PER1 was found at ZT10 and peak expression of PER2 at ZT15 in the SCN, in agreement with results in the mouse [24] and Lewis rats, where peak expression of PER2 occurred in the early part of the dark phase [5].

Because the SCN may hierarchically influence the subordinate oscillators [25] in several processes, desynchronization of the SCN in response to a neuroinflammatory stimulus could determine changes in the expression pattern of clock genes in other brain areas. In the present study, the differences in the LPS response pattern among the SCN, hippocampus, and cerebellum indicate a possible independence in this response without a hierarchical control of the central clock in relation to its subordinate oscillators [26].

In the present study, the neuroinflammatory stimulus resulted in variation in PER1 and PER2 expression in different layers of the hippocampus. Whether this immune system response reflects hippocampal function requires further investigation. Some studies have investigated the relationship between the hippocampus and alterations in proinflammatory cytokines, circadian rhythms and psychiatric disorders such as depression [10, 27].

The cerebellum showed PER1 and PER2 expression in the Purkinje cells, in agreement with the idea that the cerebellum oscillator possibly resides in these cells [28]. Our results showed that PER1 and PER2 expression can change in the cerebellum in a pathological condition.

Considering that various immune functions are under circadian control [11, 29], the desynchronization of circadian rhythms leads to altered inflammatory responses [30]. Here, we confirmed that immune factors are able to modulate circadian physiology acting at the principal and subordinate oscillators [31]. These conditions reinforce the idea that the immune and circadian system interact in a bidirectional manner [11, 29].

Whether the effects of LPS exposure on PER1 and PER2 expression found in the present study, not only in the SCN pacemaker but also in the subordinate oscillators, are transitory and whether therapeutics could be used to reestablish the normal phase relationship remain to be answered and could be important for the prevention and/or treatment of inflammatory diseases.

Acknowledgments

This work was supported by funding from the Fundação de Amparo à Pesquisa do Estado de São Paulo (FAPESP) research grant to L.P. (2011/51495-4) and (2017/23539-3).

Disclosure Statement

The authors declare that they have no conflicts of interest.

References

1 Lowrey PL, Takahashi JS: Genetics of the mammalian circadian system: photic entrainment, circadian pacemaker mechanisms, and posttranslational regulation. Annu Rev Genet 2000;34:533–562.

2 Bae K, Jin X, Maywood ES, Hastings MH, Reppert SM, Weaver DR: Differential functions of mPer1, mPer2, and mPer3 in the SCN circadian clock. Neuron 2001;30:525–536.

3 Chun LE, Woodruff ER, Morton S, Hinds LR, Spencer RL: Variations in phase and amplitude of rhythmic clock gene expression across prefrontal cortex, hippocampus, amygdala, and hypothalamic paraventricular and suprachiasmatic nuclei of male and female rats. J Biol Rhythms 2015;30:417–436.

4 Lamont EW, Robinson B, Stewart J, Amir S: The central and basolateral nuclei of the amygdala exhibit opposite diurnal rhythms of expression of the clock protein Period2. Proc Natl Acad Sci USA 2005;102:4180–4184.

5 Harbour VL, Weigl Y, Robinson B, Amir S: Phase differences in expression of circadian clock genes in the central nucleus of the amygdala, dentate gyrus, and suprachiasmatic nucleus in the rat. PLoS One 2014;9:e103309.

6 Okada K, Yano M, Doki Y, Azama T, Iwanaga H, Miki H, Nakayama M, Miyata H, Takiguchi S, Fujiwara Y, Yasuda T, Ishida N, Monden M: Injection of LPS causes transient suppression of biological clock genes in rats. J Surg Res 2008;145:5–12.

7 Cavadini G, Petrzilka S, Kohler P, Jud C, Tobler I, Birchler T, Fontana A: TNF-alpha suppresses the expression of clock genes by interfering with E-box-mediated transcription. Proc Natl Acad Sci USA 2007;104:12843–12848.
8 Yamamura Y, Yano I, Kudo T, Shibata S: Time-dependent inhibitory effect of lipopolysaccharide injection on Per1 and Per2 gene expression in the mouse heart and liver. Chronobiol Int 2010;27:213–232.
9 Haimovich B, Reddell MT, Calvano JE, Calvano SE, Macor MA, Coyle SM, Lowry SF: A novel model of common Toll-like receptor 4- and injury-induced transcriptional themes in human leukocytes. Crit Care 2010;14:R177.
10 Guan XT, Lin WJ, Tang MM: Comparison of stress-induced and LPS-induced depressive-like behaviors and the alterations of central proinflammatory cytokines mRNA in rats. Psych J 2015;4:113–122.
11 Prendergast BJ, Cable EJ, Stevenson TJ, Onishi KG, Zucker I, Kay LM: Circadian disruption alters the effects of lipopolysaccharide treatment on circadian and ultradian locomotor activity and body temperature rhythms of female Siberian hamsters. J Biol Rhythms 2015;30:543–556.
12 Gibbs JE, Ray DW: The role of the circadian clock in rheumatoid arthritis. Arthritis Res Ther 2013;15:205.
13 Pinato L, da Silveira Cruz-Machado S, Franco DG, Campos LMG, Cecon E, Fernandes PA, Bittencourt JC, Markus RP: Selective protection of the cerebellum against intracerebroventricular LPS is mediated by local melatonin synthesis. Brain Struct Funct 2015;220:827–840.
14 Markus RP, Ferreira ZS, Fernandes PA, Cecon E: The immune-pineal axis: a shuttle between endocrine and paracrine melatonin sources. Neuroimmunomodulation 2007;14:126–133.
15 Kluger MJ: Fever: role of pyrogens and cryogens. Physiol Rev 1991;71:93–127.
16 Banks WA, Gray AM, Erickson MA, Salameh TS, Damodarasamy M, Sheibani N, Meabon JS, Wing EE, Morofuji Y, Cook DG, Reed MJ: Lipopolysaccharide-induced blood-brain barrier disruption: roles of cyclooxygenase, oxidative stress, neuroinflammation, and elements of the neurovascular unit. J Neuroinflammation 2015;12:223.
17 Shi J, Zhao Y, Wang Y, Gao W, Ding J, Li P, Hu L, Shao F: Inflammatory caspases are innate immune receptors for intracellular LPS. Nature 2014;514:187–192.
18 Remick DG, Newcomb DE, Bolgos GL, Call DR: Comparison of the mortality and inflammatory response of two models of sepsis: lipopolysaccharide versus cecal ligation and puncture. Shock 2000;13:110–116.
19 Campos LM, Cruz-Rizzolo RJ, Watanabe IS, Pinato L, Nogueira MI: Efferent projections of the suprachiasmatic nucleus based on the distribution of vasoactive intestinal peptide (VIP) and arginine vasopressin (AVP) immunoreactive fibers in the hypothalamus of *Sapajus apella*. J Chem Neuroanat 2014;57–58:42–53.
20 Yu X, Li Z, Zheng H, Ho J, Chan MT, Wu WK: Protective roles of melatonin in central nervous system diseases by regulation of neural stem cells. Cell Prolif 2017;50:e12323.
21 Marpegán L, Bekinschtein TA, Costas MA, Golombek DA: Circadian responses to endotoxin treatment in mice. J Neuroimmunol 2005;160:102–109.
22 Guerrero-Vargas NN, Salgado-Delgado R, Basualdo Mdel C, García J, Guzmán-Ruiz M, Carrero JC, Escobar C, Buijs RM: Reciprocal interaction between the suprachiasmatic nucleus and the immune system tunes down the inflammatory response to lipopolysaccharide. J Neuroimmunol 2014;273:22–30.
23 Smolensky MH, Lemmer B, Reinberg AE: Chronobiology and chronotherapy of allergic rhinitis and bronchial asthma. Adv Drug Deliv Rev 2007;59:852–882.
24 O'Callaghan EK, Anderson ST, Moynagh PN, Coogan AN: Long-lasting effects of sepsis on circadian rhythms in the mouse. PLoS One 2012;7:e47087.
25 Ralph MR, Foster RG, Davis FC, Menaker M: Transplanted suprachiasmatic nucleus determines circadian period. Science 1990;247:975–978.
26 Stoynev AG, Ikonomov OC, Damova IA, Penev PD, Usunoff KG, Paloff AM: Suprachiasmatic nuclei lesions eliminate light/dark variations in short-term feeding responses to deprivation or insulin treatment in rats. Physiol Behav 1990;48:795–799.
27 Moriya S, Tahara Y, Sasaki H, Hamaguchi Y, Kuriki D, Ishikawa R, Ishigooka J, Shibata S: Effect of quetiapine on Per1, Per2, and Bmal1 clock gene expression in the mouse amygdala and hippocampus. J Pharmacol Sci 2014;125:329–332.
28 Mordel J, Karnas D, Pévet P, Isope P, Challet E, Meissl H: The output signal of Purkinje cells of the cerebellum and circadian rhythmicity. PLoS One 2013;8:e58457.
29 Curtis AM, Fagundes CT: Understanding the role of cellular molecular clocks in controlling the innate immune response. Methods Mol Biol 2016;1390:301–316.
30 Castanon-Cervantes O, Wu M, Ehlen JC, Paul K, Gamble KL, Johnson RL, Besing RC, Menaker M, Gewirtz AT, Davidson AJ: Dysregulation of inflammatory responses by chronic circadian disruption. J Immunol 2010;185:5796–5805.
31 Logan RW, Sarkar DK: Circadian nature of immune function. Mol Cell Endocrinol 2012;349:82–90.